Journal of Magnetic Resonance **151,** 339–346 (2001)
doi:10.1006/jmre.2001.2376, available online at http://www.idealibrary.com on IDEAL®

# COMMUNICATIONS

# Measuring the Longitudinal NMR Relaxation Rates of Fast Relaxing Nuclei Using a Signal Eliminating Relaxation Filter

D. Flemming Hansen and Jens J. Led[1]

*Department of Chemistry, University of Copenhagen, The H. C. Ørsted Institute, Universitetsparken 5, DK-2100 Copenhagen Ø, Denmark*

Received March 2, 2001; revised April 25, 2001; published online July 3, 2001

**A new experiment for selective determination of the relaxation rates of fast relaxing NMR signals is presented. The experiment is derived from the conventional inversion recovery experiment by substituting the 180° inversion pulse of this experiment with a signal eliminating relaxation filter (SERF) consisting of three 180° pulses separated by two variable delays, $\Delta_1$ and $\Delta_2$. The SERF experiment allows a selective suppression of signals with relaxation rates below a given limit while monitoring the relaxation of faster relaxing signals. The experiment was tested on a sample of 20% oxidized plastocyanin from *Anabaena variabilis*, where the fast exchange of an electron between the reduced (diamagnetic) and the oxidized (paramagnetic) form results in a series of average signals with widely different relaxation rates. To ensure an optimum extraction of information from the experimental data, the relaxation rates were obtained from the SERF experiment by a simultaneous analysis of all the FIDs of the experiment using a fast linear prediction model method developed previously. The reliability of the relaxation rates obtained from the SERF experiment was confirmed by a comparison of the rates with the corresponding rates obtained from a conventional inversion recovery experiment.** 

*Key Words*: **SERF experiment; relaxation filter; linear prediction; paramagnetic relaxation;** *Anabaena variabilis* **plastocyanin.**

## INTRODUCTION

Determination of the longitudinal relaxation rates $R_1$ of fast relaxing nuclear spin plays an important role in studies of the structure and function of paramagnetic metallo-proteins (*1–3*). Thus, dipolar and scalar interactions of the nuclei with the unpaired metal-electrons can give rise to significant enhancements of the nuclear relaxation which, in turn, can provide valuable information about the geometric and electronic structures of the proteins. In particular, information about the relaxation of nuclei spatially close to the metal ion is important for mapping the structure of the metal site and elucidating the functional mechanisms of the protein.

Unfortunately, the longitudinal relaxation rates of the nuclei close to the metal center are the most difficult to measure by the conventional $R_1$ relaxation experiments because of poor resolution caused by severe line broadening and signal overlap. The super-WEFT experiment (*4, 5*) alleviates the resolution problem by allowing observation only of resonances with fast longitudinal relaxation while suppressing the slow relaxing signals. This virtue of the super-WEFT experiment was recently exploited in a study of the electron self-exchange rate of plastocyanin from *Anabaena variabilis* (*6*), where the self-exchange rate was determined from the linewidths of signals in a $^1$H super-WEFT spectrum of the protein.

Still, the super-WEFT technique cannot be used for measuring fast $R_1$ relaxation rates. This holds since both the relaxation delay, $t_b$, and the acquisition delay, $t_a$, in the super-WEFT pulse sequence, $180^\circ - t_b - 90^\circ - t_a$, must remain constant throughout the experiment to ensure an unchanged saturation of the slow relaxing signals. That is, in the super-WEFT experiment, the condition

$$e^{-t_a R_1^s} + e^{t_b R_1^s} - 2 = 0 \qquad [1]$$

must be fulfilled (*5*) at least approximately, in order for signals with the relaxation rate $R_1^s$ to be suppressed. On the other hand, monitoring the decay of fast relaxing signals requires a variation of the delay $t_b$ as well as a constant acquisition time, $t_a$, as in the inversion recovery (IR) relaxation experiment (*7*). Consequently $R_1$ rates cannot be determined using the super-WEFT experiment.

Here we present a new experiment for selective determination of the relaxation rates of fast relaxing signals. The experiment is based on a signal eliminating relaxation filter (SERF) that allows a variable delay for monitoring the relaxation of the fast relaxing signals, as in the IR experiment, while retaining the capability of the super-WEFT experiment to suppress slow relaxing signals.

## THEORY

Basically the SERF experiment is derived from the conventional inversion recovery (IR) experiment (*7*) by substituting the 180° inversion pulse with three 180° pulses separated by

[1]To whom correspondence should be addressed.



1090-7807/01 $35.00

two variable delays, $\Delta_1$ and $\Delta_2$, that is

$$180^\circ - \Delta_1 - 180^\circ - \Delta_2 - 180^\circ - \tau - 90^\circ - t_a. \quad [2]$$

As shown below, proper adjustment of the delays, $\Delta_1$ and $\Delta_2$, in conjunction with a systematic variation of the relaxation delay $\tau$, allows a constant saturation of the slow relaxing NMR signals, while monitoring the exponential recovery of the fast relaxing signals. In the following it is assumed that the transverse magnetization has vanished at the end of the $\tau$ delay resulting in a negligible longitudinal magnetization after the 90° pulse. Further it is assumed that steady-state magnetization is achieved at the end of the acquisition period, $t_a$, after a number of dummy scans (*5*). Finally, it is assumed that the applied pulses are ideal 180° or 90° pulses.

Under these conditions the longitudinal magnetization immediately after the acquisition period (Eq. [2]) is given by

$$\frac{M_z}{M_z^\infty} = 1 - e^{-R_1 t_a} \quad [3]$$

according to the Bloch equation (*9*). Here $M_z^\infty$ is the equilibrium magnetization, and $R_1$ is the longitudinal relaxation rate. Similarly the magnetization at the start of the $\tau$ delay can be derived by applying the Bloch equation to the sequence $t_a - 180^\circ - \Delta_1 - 180^\circ - \Delta_2 - 180^\circ$, that is

$$\frac{M_z}{M_z^\infty} = e^{-R_1(t_a+\Delta_1+\Delta_2)} - 2e^{-R_1(\Delta_1+\Delta_2)} + 2e^{-R_1\Delta_2} - 1. \quad [4]$$

Furthermore, the magnetization immediately before the 90° pulse and, thereby, the intensity of the observed resonance is given by

$$\frac{M_z}{M_z^\infty} = e^{-R_1(t_a+\Delta_1+\Delta_2+\tau)} - 2e^{-R_1(\Delta_1+\Delta_2+\tau)} + 2e^{-R_1(\Delta_2+\tau)} - 2e^{-R_1\tau} + 1. \quad [5]$$

For the suppressed signals, the magnetization at the beginning of the acquisition period (Eq. [5]) must be zero; that is

$$e^{-R_1^s(t_a+\Delta_1+\Delta_2+\tau)} - 2e^{-R_1^s(\Delta_1+\Delta_2+\tau)} + 2e^{-R_1^s(\Delta_2+\tau)} - 2e^{-R_1^s\tau} + 1 = 0 \quad [6]$$

or

$$\left(e^{-R_1^s t_a} - 2\right) e^{-R_1^s\Delta_1} - \left(2 - e^{R_1^s\tau}\right) e^{R_1^s\Delta_2} + 2 = 0, \quad [7]$$

where $R_1^s$ is the relaxation rate of the suppressed signals. Thus, signals with relaxation rates equal or close to $R_1^s$ vanish or are suppressed significantly for values of $\Delta_1$ and $\Delta_2$ that fulfill Eq. [7].

For the observed signals, the magnetization at the beginning of the relaxation delay $\tau$ (Eq. [4]) must assume the same value independent of $\tau$ to ensure a single-exponential decay of the observed longitudinal magnetization. This condition is fulfilled if $dM_z = 0$, where $dM_z$ is the dependence of the longitudinal magnetization on $\Delta_1$, $\Delta_2$, and $t_a$ at the start of the $\tau$ delay (Eq. [4]), that is

$$dM_z = \left(\frac{\partial M_z}{\partial \Delta_1}\right)_{\Delta_2,t_a} d\Delta_1 + \left(\frac{\partial M_z}{\partial \Delta_2}\right)_{\Delta_1,t_a} d\Delta_2 + \left(\frac{\partial M_z}{\partial t_a}\right)_{\Delta_1,\Delta_2} dt_a. \quad [8]$$

Since $t_a$ is unchanged throughout the experiment, Eq. [8] reduces to

$$dM_z = \left(\frac{\partial M_z}{\partial \Delta_1}\right)_{\Delta_2} d\Delta_1 + \left(\frac{\partial M_z}{\partial \Delta_2}\right)_{\Delta_1} d\Delta_2. \quad [9]$$

For $dM_z = 0$, Eq. [9] gives

$$\frac{d\Delta_2}{d\Delta_1} = -\left(\frac{\partial M_z}{\partial \Delta_1}\right)_{\Delta_2} \Big/ \left(\frac{\partial M_z}{\partial \Delta_2}\right)_{\Delta_1}. \quad [10]$$

From Eq. [4] the following two relations can be obtained,

$$\left(\frac{\partial M_z}{\partial \Delta_1}\right)_{\Delta_2} = M_z^\infty \left(2R_1 e^{-R_1(\Delta_1+\Delta_2)} - R_1 e^{-R_1(t_a+\Delta_1+\Delta_2)}\right) \quad [11]$$

and

$$\left(\frac{\partial M_z}{\partial \Delta_2}\right)_{\Delta_1} = M_z^\infty \left(2R_1 e^{-R_1(\Delta_1+\Delta_2)} - R_1 e^{-R_1(t_a+\Delta_1+\Delta_2)} - 2R_1 e^{-R_1\Delta_2}\right). \quad [12]$$

Using Eqs. [11] and [12], Eq. [10] can be written as

$$\frac{d\Delta_2}{d\Delta_1} = \frac{e^{-R_1^o t_a} - 2}{2 - e^{-R_1^o t_a} - 2e^{R_1^o\Delta_1}}, \quad [13]$$

where $R_1^o$ is the relaxation rate of the observed protons. Finally, integration of Eq. [13] gives

$$\left(1 - 2e^{R_1^o t_a}\right) e^{-R_1^o\Delta_1} - e^{-c} e^{R_1^o\Delta_2} + 2e^{R_1^o t_a} = 0, \quad [14]$$

where $c$ is a constant of integration. The value of $c$ determines the $\tau$ range for optimum suppression and can be chosen accordingly, as illustrated below. Thus, for specific values of $R_1^s$, $R_1^o$, and $c$ a set of $\Delta_1$ and $\Delta_2$ delays, that fulfill the saturation and relaxation requirements mentioned above, can be found for each $\tau$ value in a relaxation experiment by solving Eqs. [7] and [14]

simultaneously. Note that in extreme cases where $R_1^o$ and $R_1^s$ are close to one another Eqs. [7] and [14] may not have a simultaneous solution.

## EXPERIMENTAL PROCEDURES

### *Sample Preparation*

Plastocyanin from *Anabaena variabilis* (*A.v.* PCu) was prepared and purified as described previously (*10*). The protein was dissolved in 99.9% $D_2O$ at pH 7.16 (meter reading) and a concentration of 1.89 mM. A sample containing approximately 20% of the oxidized (paramagnetic) form (PCu(II)/PCu(I) $\approx$ 20%/80%) was prepared by adding the proper amount of $K_3[Fe(CN)_6]$ to a sample of the reduced (diamagnetic) form.

### *NMR Experiments*

All spectra were recorded at 298 K and a $^1H$ frequency of 500 MHz using a Varian Unity Inova 500 spectrometer. The $^1H$ carrier was placed on the HDO signal (4.77 ppm relative to TMS at 298 K (*11*)). The spectral width was 8000 Hz in the SERF experiments and 9000 Hz in the IR experiments. Fourteen relaxation delays, $\tau$, ranging from 1 to 90 ms were used in both types of experiment, allowing the determination of $R_1$ rates in the range from 35 to 200 $s^{-1}$. In the inversion recovery experiments each spectrum consisted of 32 scans preceded by 8 dummy scans to achieve steady state condition, while the acquisition time was 1.820 s. In the SERF experiments, 512–4000 scans were used for each spectrum, while the number of dummy scans was 128–512 and the acquisition time was 70 ms. Sets of $\Delta_1$ and $\Delta_2$ delays corresponding to the $\tau$ values were calculated as described in the theory section. Typical sets of delays (used to obtain the spectra in Fig. 5) are given in Table 1.

### *Data Analysis Using the Linear Prediction Model Method*

A direct fit to the FIDs of a model that describes the FIDs and their dependence on the $R_1$ rates would be the optimum approach for analyzing the SERF experiment or any other experiment consisting of a series of FIDs. Thus, for spectra with $n$ signals the entire set of FIDs as a function of the sampling time, $t$, and the delay time, $\tau$, is given by

$$FID(\tau, t) = \sum_{k=1}^{n} \left[ I_k^\infty - \left( I_k^\infty - I_k^0 \right) e^{-R_{1,k}\tau} \right] \times \exp\{(2\pi i \nu_k - \pi \Delta\nu_{1/2,k})t + i\phi_k\}, \quad [15]$$

where $I_k^\infty$ is the equilibrium intensity of the $k$th signal, $I_k^0$ is the initial intensity, $R_{1,k}$ is the relaxation rate, $\nu_k$ is the frequency, $\Delta\nu_{1/2,k}$ is the linewidth, and $\phi_k$ is the phase of the $k$th signal.

In practice, this direct approach is not possible since the number of signals ($n$) in the spectra is unknown *a priori*. Neither is it feasible because of the very large amount of data involved in the analysis. Both of these problems are alleviated by the linear prediction model method described previously (*12*). The first step of this method is a fast linear prediction (FLP) analysis (*13*) of the individual FIDs corresponding to the different $\tau$ delays. This analysis provides not only the number of signals in the spectra, but also estimates of the four spectral parameters of each of the $n$ signals predicted by the FLP analysis. These parameters are the intensity, $I_k(\tau)$, the frequency, $\nu_k$, the linewidth, $\Delta\nu_{1/2,k}$, and the phase, $\phi_k$, as well as the uncertainties and the correlations of these parameters. Thus, the FLP analysis transfers all the information contained in the spectra to the $4 \times n$ spectral parameters and the uncertainties and correlations obtained by the analysis.

However, the number of signals found by the FLP calculations may vary from one FID to another, or the intensities of the predicted signals are heavily correlated because of severe overlap. Therefore, the estimated intensities of closely spaced signals are often distributed in an unpredictable way among the signals. Consequently, a direct fit of the exponential decay of the $R_1$ relaxation to the time dependence of the intensities would be difficult and would probably lead to erroneous results.

This problem can be overcome by creating a set of auxiliary FIDs from the spectral parameters obtained by the FLP analysis. Thus, for each experimental FID an auxiliary FID is created corresponding to a specific spectral region of interest. Each auxiliary FID consists of a number of points (the $t$ values in Eq. [15]) equal to the number of parameters describing the specific spectral region. The amount of data involved can, thereby, be reduced substantially, making the analysis feasible. Still the information contained in the auxiliary FIDs is exactly the same as in the spectral parameters or in the original experimental data that describes the region.

Subsequently, the six model parameters (Eq. [15]) for each of the $n$ signals, that is, the relaxation rates $R_{1,k}$ and the model parameters $I_k^0$, $I_k^\infty$, $\nu_k$, $\Delta\nu_{1/2,k}$, and $\phi_k$, can be determined by a simultaneous nonlinear least squares fit of Eq. [15] to the complete set of auxiliary FIDs. These $6 \times n$ model parameters describe the physics of the system, and their estimated values contain all the information of the experimental spectra. Furthermore, reliable estimates are ensured not only of the model

**TABLE 1**
**Typical Delays Used in the SERF Pulse Sequence[a]**

| Spectra | $\Delta_1$/s | $\Delta_2$/s | $\tau$/s |
|---|---|---|---|
| a | 0.0664 | 0.1156 | 0.0905 |
| b | 0.1406 | 0.1182 | 0.0453 |
| c | 0.1782 | 0.1183 | 0.0226 |
| d | 0.2069 | 0.1184 | 0.0057 |
| e | 0.2150 | 0.1184 | 0.0010 |

[a] Used to obtain the SERF spectra in Fig. 5. The delays were calculated from Eqs. [7] and [14] using the parameters $R_1^o = 35\ s^{-1}$, $R_1^s = 2\ s^{-1}$, $c = 1.0$, $t_a = 70$ ms and the $\tau$ delays indicated in Fig. 5.

parameters but also of their standard deviations, since the standard deviations and the correlations determined by the FLP analysis are included in the nonlinear least squares fit of Eq. [15]. Thus, the linear prediction model method provides the optimum approach for analyzing the SERF experiment. It should be emphasized that the approach is generally applicable to simultaneous analyses of series of experimental FIDs, whenever the variation among the FIDs can be described by a mathematical model.

## RESULTS AND DISCUSSION

As described in the Theory section a complete $^1$H SERF experiment comprises a series of one-dimensional spectra with different $\tau$ delays, each with a corresponding set of $\Delta_1$ and $\Delta_2$ delays. Calculation of the $\Delta_1$ and $\Delta_2$ delays (Eqs. [7] and [14] ) requires typical values of the acquisition time $t_a$ and the constant $c$ in addition to the $\tau$ delay. Furthermore, a set of reasonable values of $R_1^o$ and $R_1^s$ are required and must be assumed, $R_1^o$ and $R_1^s$ being typical relaxation rates of the signals to be observed and suppressed, respectively. In order to investigate the applicability of the SERF experiment, a series of simulations using typical values of the parameters $R_1^o$, $R_1^s$, $t_a$, $c$, and $\tau$ was made, as described below.

### *The Relaxation Selectivity of the SERF Experiment*

For the observable protons the magnetization immediately before the relaxation $\tau$ delay (Eq. [4]) must assume the same value independent of the $\tau$ delay, as discussed in theory. This condition is fulfilled exactly for protons with relaxation rates equal to the assumed $R_1^o$ rate used in the calculation of the $\Delta_1$ and $\Delta_2$, and, to a close approximation for protons with relaxation rates faster than the assumed $R_1^o$ rate. This is shown in Fig. 1,

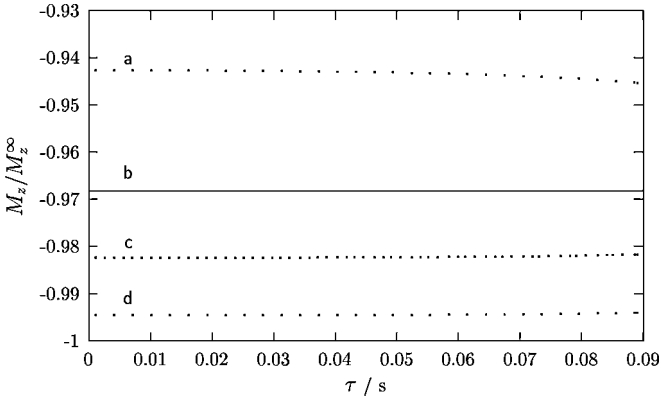


**FIG. 1.** Simulation of the longitudinal magnetization of the observed signals immediately before the $\tau$ delay (Eq. [4]) using the parameters $R_1^o = 35\ s^{-1}$, $R_1^s = 2\ s^{-1}$, $c = 1.0$, and $t_a = 70$ ms. Simulations are shown for signals with relaxation rates close to or equal to $R_1^o$, that is (a) $R_1 = 30\ s^{-1}$; (b) $R_1 = 35\ s^{-1}$; (c) $R_1 = 40\ s^{-1}$; and (d) $R_1 = 50\ s^{-1}$.

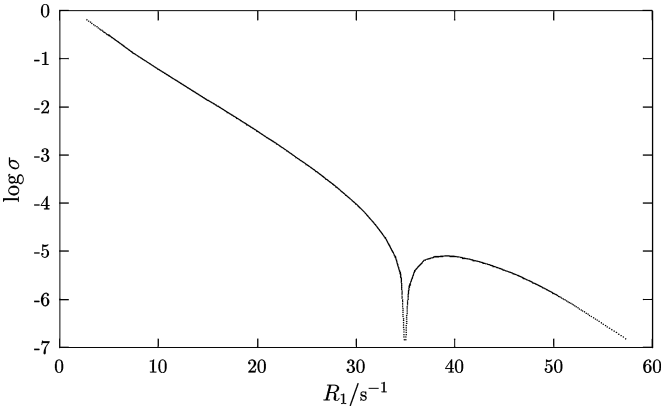


**FIG. 2.** Simulation of the systematic relative error, $\sigma$, of the obtained $R_1$ rates caused by nonexponential decays (see text). The following parameters were used: $R_1^o = 35\ s^{-1}$, $R_1^s = 2\ s^{-1}$, $c = 1.0$, and $t_a = 70$ ms.

where the intensity as function of the $\tau$ delay is given for a series of signals with $R_1$ rates equal or close to $35\ s^{-1}$. The intensities were calculated using Eq. [4], while the $\Delta_1$ and $\Delta_2$ delays were obtained from Eqs. [7] and [14] using $R_1^o = 35\ s^{-1}$, $R_1^s = 2\ s^{-1}$, $c = 1$, $t_a = 70$ ms, and the $\tau$ delays given in Fig. 1. As it appears from Fig. 1, the condition of constant magnetization is approximately fulfilled also for relaxation rates slower than $35\ s^{-1}$. Consequently, also these rates can be estimated from the experimental data using Eq. [15], although a minor systematic error appears if the derived relaxation rates deviate significantly from the assumed $R_1^o$, as discussed below.

The systematic error occurs because the decay of the observed magnetization $M_z(\tau)$ (Eq. [5]) is only approximately single-exponential when the relaxation rate deviates from $R_1^o$. To estimate the error, magnetization decays corresponding to $R_1$ rates in the vicinity of $R_1^o = 35\ s^{-1}$ were calculated using Eq. [5] and the same $\Delta_1$ and $\Delta_2$ delays as above. Subsequently, the calculated magnetizations were fitted by a single-exponential decay, and the obtained relaxation rates $R_1^{fit}$ were used to calculate the fractional deviation $\sigma$:

$$\sigma = \frac{\left|R_1 - R_1^{fit}\right|}{R_1}. \qquad [16]$$

It should be noted that $R_1^{fit} > R_1$ for $R_1 < R_1^o$, while $R_1^{fit} < R_1$ for $R_1 > R_1^o$. As shown in Fig. 2, the deviations are small in particular for $R_1 > R_1^o$. For $R_1 < R_1^o$, the error increases with decreasing relaxation rates while, at the same time, the signal intensities decrease because of the suppression. Thus for example, for $R_1 = 10\ s^{-1}$ the systematic error is about 6% while the intensity is only 43%. In principle, the use of Eq. [5] in the data analysis instead of a simple single-exponential decay should eliminate the systematic error, although it is at the expense of simplicity in the analysis.

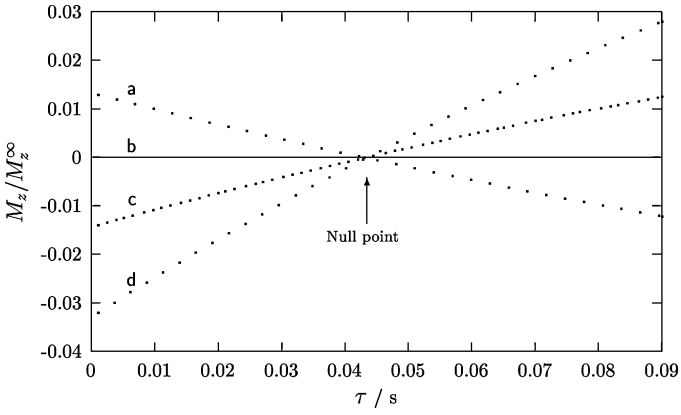


**FIG. 3.** Simulation of the longitudinal magnetization immediately before the 90° pulse (Eq. [5]) using the parameters $R_1^o = 35\ s^{-1}$, $R_1^s = 2\ s^{-1}$, $c = 1.0$, and $t_a = 70$ ms. The suppression is shown for signals with relaxation rates close to $R_1^s$. (a) $R_1 = 1\ s^{-1}$; (b) $R_1 = 2.0\ s^{-1}$; (c) $R_1 = 2.5\ s^{-1}$; (d) $R_1 = 3\ s^{-1}$.

### *The Suppression Efficiency of the SERF Experiment*

The intensities of the suppressed signals in the SERF spectra were calculated from Eq. [5] using the same $\Delta_1$ and $\Delta_2$ delays as in the above investigation of the relaxation selectivity. The results are given in Fig. 3, which shows the intensities of signals with relaxation rates in the vicinity of $2\ s^{-1}$. As it appears from Fig. 3 the suppression is most effective at the "null point" and less effective for large $\tau$ values and for $\tau \to 0$. The position of the null point can be changed by adjusting the constant $c$ in Eq. [14]. The optimum value of $c$ is obtained when the null point appears in the middle of the applied $\tau$ interval, making the overall suppression most effective.

An important feature shown in Fig. 3 is the variation of the intensities of the small signals from protons with relaxation rates slower than $R_1^s$. These intensities are *positive* when $\tau \to 0$ while *negative* for large values of $\tau$. Thus, for the same values of $R_1^o$, $R_1^s$, $c$, and $t_a$ as above and in Fig. 1, the signals from protons with relaxation rates of $1\ s^{-1}$ are suppressed to approximately 1% *and* have an orientation opposite those of the fast relaxing protons, thereby making the observation of the latter protons easier.

It also appears from Fig. 3 that the suppression is less effective for large $\tau$ values and for $\tau \to 0$. A lower limit for the suppression in a $^1$H SERF experiment can, therefore, be estimated from the suppression at $\tau = 0$. This is shown in Fig. 4, where the suppression is calculated for three different experiments. In all three cases the constant $c$ is chosen so that the null point corresponds to $\tau = 45$ ms, that is, in the middle of the applied $\tau$ interval. As it appears from a and c in Fig. 4, changing $R_1^s$ from 2 to $3\ s^{-1}$ with constant $R_1^o$ and $t_a$ results in a less effective suppression of signals with $0\ s^{-1} \le R_1 \le 2.5\ s^{-1}$. That is, a larger range of suppression results in a less effective overall suppression. Furthermore, it appears from b and c in Fig. 4 that the suppression is less effective for longer acquisition times. That is, for a constant spectral width an attempt to increase the resolution by extending $t_a$ will result in a less effective suppression.

Finally it should be noted that suppression of slow relaxing signals in the SERF experiment is superior to the suppression obtained in an alternative phase cycling filter experiment, i.e., $180^\circ_x - \Delta - 90^\circ_x 90^\circ_{x,-x} - \tau - 90^\circ_x - t_a$, receiver $(x, -x)$, where $\Delta = \ln 2/R_1^s$ so that the phase-cycled 90° pulse is applied at the zero crossing of the suppressed spin. A simple calculation shows that protons with relaxation rates between 1 and $3\ s^{-1}$ are suppressed only to approximately 35% of their original intensity in a phase cycling filter experiment optimized to suppress signals with relaxation rates of about $2\ s^{-1}$. A comparison of this result with the suppression shown in Fig. 3 clearly illustrates the superiority of the SERF experiment.

### *Experimental Verification*

An experimental verification of the SERF experiment was made using the 20% oxidized *A.v.* PCu sample described in the Experimental section. The paramagnetic $Cu^{2+}$ ion in the oxidized form of this protein, and its fast electron self-exchange rate (approximately $400\ s^{-1}$ at the applied experimental conditions (*6*)) ensure a fast relaxation of the observed average signals of protons spatially close to the copper ion, while protons at larger distances are slow relaxing.

In Fig. 5, a spectrum from the SERF experiment performed on *A.v.* PCu is compared with the corresponding regular one-dimensional $^1$H spectrum. The assignments shown in Fig. 5a were obtained previously (*2*, *10*). The total acquisition time was 1 h in both experiments. The SERF spectrum was recorded with 512 scans and 128 dummy scans while the regular $^1$H spectrum consists of only 32 scans and 8 dummy scans. The different number of scans results from the different repetition rates of the two

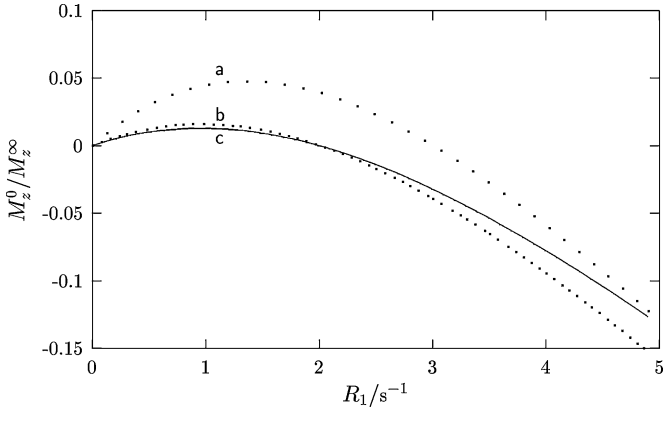


**FIG. 4.** Simulation showing the suppression as function of $R_1$ for three different experiments; (a) $R_1^o = 35\ s^{-1}$, $R_1^s = 3\ s^{-1}$, $t_a = 70$ ms, and $c = 1.5$; (b) $R_1^o = 35\ s^{-1}$, $R_1^s = 2\ s^{-1}$, $t_a = 90$ ms, and $c = 0.8$; (c) $R_1^o = 35\ s^{-1}$, $R_1^s = 2\ s^{-1}$, $t_a = 70$ ms, and $c = 1$. In all experiments the constant $c$ was chosen so that the null point appears for $\tau = 45$ ms, that is, in the middle of the applied $\tau$ interval.

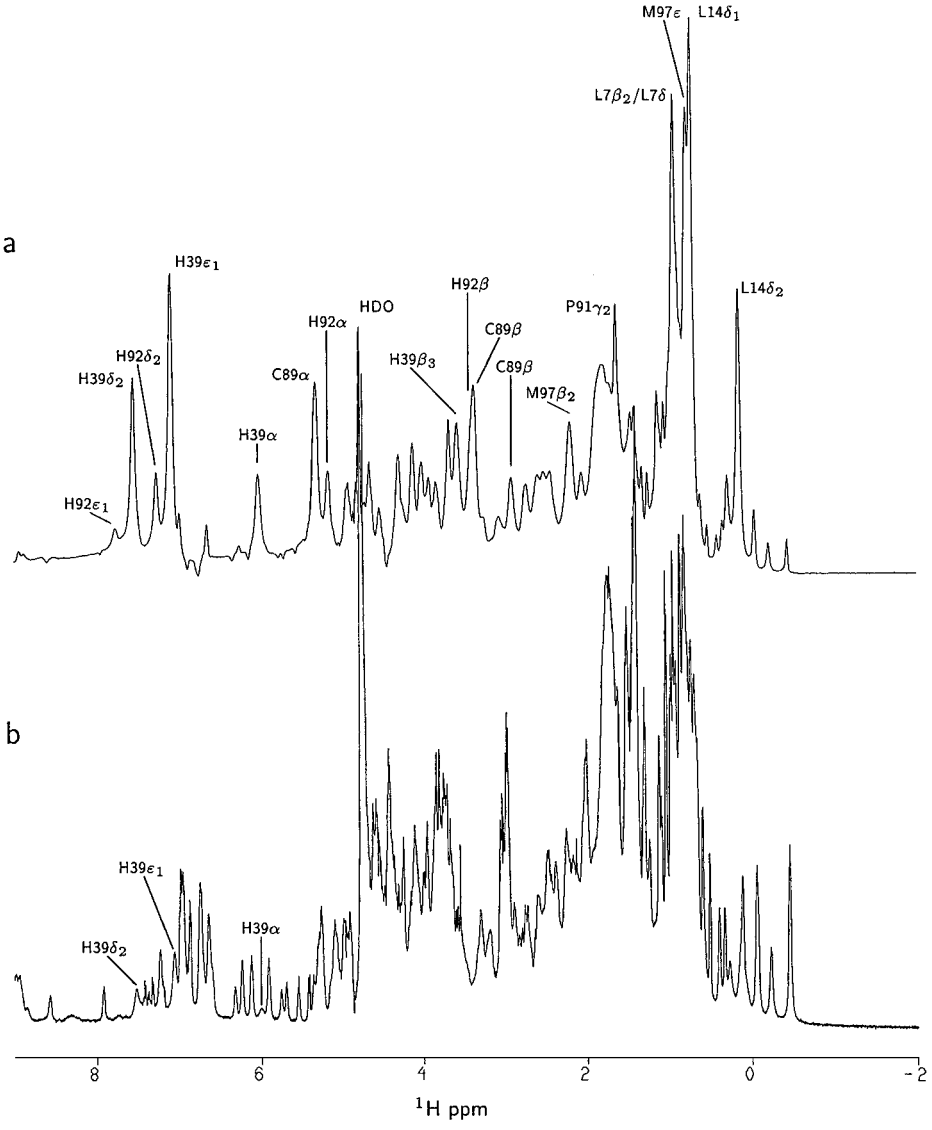


**FIG. 5.** Comparison of (a) a $^1$H SERF spectrum and (b) a regular $^1$H spectrum of an approximately 20% oxidized sample of 1.89 mM (*A.v.* PCu in 99.9% $D_2O$ at pH 7.16, meter reading). The $\Delta_1$ and $\Delta_2$ delays used to record the $^1$H SERF spectrum were calculated from Eqs. [7] and [14] using the parameters $R_1^o = 35\ s^{-1}$, $R_1^s = 2\ s^{-1}$, $c = 1.0$, $t_a = 70$ ms, and $\tau = 90.5$ ms, corresponding to the longest $\tau$ delay. A total of 512 scans were used, while 128 dummy scans were applied prior to acquisition. The $^1$H spectrum was recorded with a saturation delay of 6 s, $\tau = 8$ s, and an acquisition time of 1.820 s. All signals observed in the $^1$H SERF spectrum are from protons with fast relaxation rates, i.e., spatial close to the paramagnetic Cu(II).

experiments. As it appears from a comparison of the two spectra, the slow relaxing signals are effectively suppressed in the SERF spectrum resulting in the observation of only the fast relaxing signals, as in a super-WEFT spectrum. Also, the intense HDO signal is effectively suppressed by the SERF pulse sequence.

The recovery of the fast relaxing signals observed in the SERF experiment is shown in Fig. 6, while a series of relaxation rates determined by the experiment is given in Table 2. The null point was chosen at $\tau = 45.3$ ms, resulting in the most efficient suppression for this $\tau$ delay (see Fig. 3). This is clearly observed in Fig. 6, especially in the 4.8 to 9.0 ppm range. In spectra with $\tau$ delays different from 45.3 ms smaller peaks appear from slow relaxing signals.

The opposite dependence of the slow relaxing signals on the $\tau$ delay is also observed in Fig. 6. Thus, the two resonances from Phe76 $H^{\varepsilon}$ and Phe31 $H^{\varepsilon}$ at 6.14 and 6.34 ppm, respectively, are positive at short $\tau$ delays and negative at longer $\tau$ delays, as predicted in Fig. 3 for signals with relaxation rates slower than the assumed $R_1^s$. In accord with this, the relaxation rates of the two protons were found to be $0.78 \pm 0.04$ and $1.45 \pm 0.07\ s^{-1}$, respectively, in a conventional IR experiment; that is, both rates are smaller than the $R_1^s$ rate of $2.0\ s^{-1}$.

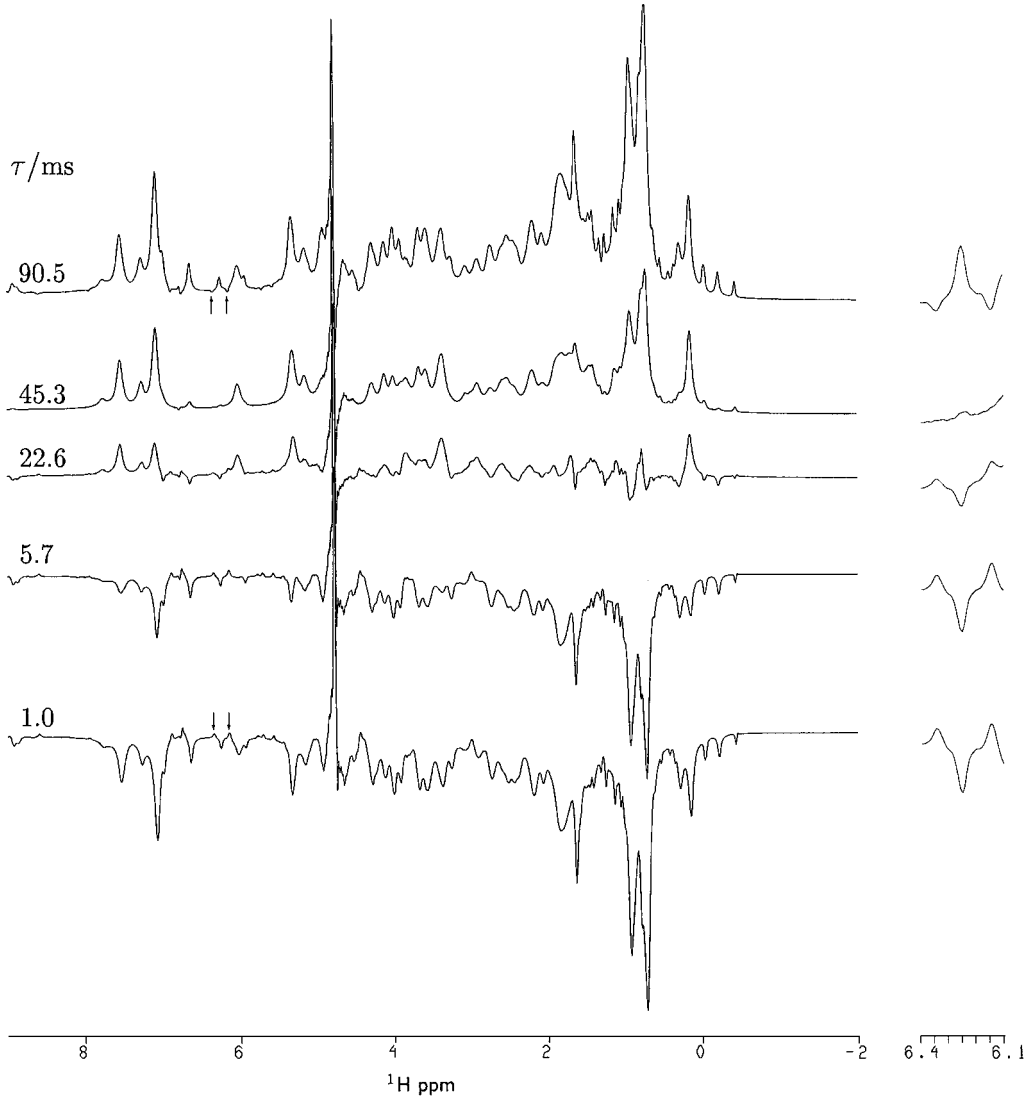


**FIG. 6.** Spectra in a $^1$H SERF experiment showing the decay of a series of fast relaxing signals in an approximately 20% oxidized sample of 1.89 mM (*A.v.* PCu in 99.9% $D_2O$ at pH 7.16, meter reading). The $\Delta_1$ and $\Delta_2$ delays used to record the $^1$H SERF spectra were calculated from Eqs. [7] and [14] using the parameters $R_1^o = 35\ s^{-1}$, $R_1^s = 2\ s^{-1}$, $c = 1.0$, $t_a = 70$ ms, and the $\tau$ delays indicated in the figure. The relaxation delay $\tau = 45.3$ ms corresponds to the null point where the suppression of the slow relaxing protons is optimum. The opposite dependence on $\tau$ of slow relaxing signals (see text) is observed for Phe76 $H^{\varepsilon}$ and Phe31 $H^{\varepsilon}$. The two signals are indicated in the spectrum ($\uparrow\uparrow$, $\downarrow\downarrow$) and shown in the excerpt (right).

**TABLE 2**
**Examples of Model Parameters Extracted from the SERF Experiment[a]**

| Nucleus | $\nu$/ppm[b] | $\Delta\nu_{1/2}$/Hz | $\phi$ | $I^0$ | $I^{\infty}$[d] | $R_1/s^{-1}$ |
|---|---|---|---|---|---|---|
| His92 $H^{\alpha}$ | $5.146 \pm 0.002$ | $54.3 \pm 1.5$ | $189 \pm 2$ | 60[c] | $67 \pm 8$ | $53 \pm 14$ |
| Cys89 $H^{\alpha}$ | $5.3109 \pm 0.0006$ | $45.3 \pm 0.6$ | $182.8 \pm 0.9$ | $-132 \pm 11$ | $134 \pm 7$ | $57 \pm 7$ |
| His39 $H^{\varepsilon_1}$ | $7.0733 \pm 0.0002$ | $42.6 \pm 0.2$ | $182.6 \pm 0.3$ | $-191 \pm 6$ | $217 \pm 8$ | $44.3 \pm 1.0$ |
| His92 $H^{\delta_2}$ | $7.2536 \pm 0.0006$ | $42.5 \pm 0.5$ | $190.8 \pm 0.9$ | $-49 \pm 6$ | 52[c] | $56 \pm 2$ |
| His39 $H^{\delta_2}$ | $7.52787 \pm 0.00015$ | $44.96 \pm 0.15$ | $183.8 \pm 0.2$ | $-99.2 \pm 1.8$ | $108.9 \pm 0.8$ | $70.4 \pm 1.8$ |
| His92 $H^{\varepsilon_1}$ | $7.7509 \pm 0.0012$ | $62.9 \pm 1.0$ | $184.6 \pm 1.6$ | 31.5[c] | $34 \pm 2$ | $37 \pm 4$ |

[a] The linear prediction model method and Eq. [15] were used to extract spectral parameters for representative excerpts of signals in Fig. 6.
[b] The uncertainty caused by the imprecise position of the $^1$H carrier on the HDO signal (4.77 ppm) is not taken into account.
[c] These parameters were fixed in the least square fit.
[d] The variation in the intensities are primarily due to negative NOEs caused by saturation of adjacent slow relaxing protons.

**TABLE 3**
**Corresponding $R_1$ Rates from the SERF and Inversion Recovery (IR) Experiments**

| | $R_1$/ s$^{-1}$ | | |
|---|---|---|---|
| Experiment | His39 H$^{\alpha}$ | His39 H$^{\delta_2}$ | His39 H$^{\varepsilon_1}$ |
| SERF[a] | $109 \pm 10$ | $70.4 \pm 1.8$ | $44.3 \pm 1.0$ |
| IR $T_1$[b] | $109 \pm 12$ | $68 \pm 10$ | $47 \pm 7$ |

[a] The $\Delta_1$ and $\Delta_2$ delays applied in the $^1$H SERF spectra were calculated from Eqs. [7] and [14] using the parameters $R_1^o = 35$ s$^{-1}$, $R_1^s = 2$ s$^{-1}$, $t_a = 70$ ms, $c = 1$ and fourteen different $\tau$ delays in the 1 to 90 ms range.

[b] The pulse sequence $sat - 180^\circ - \tau - 90^\circ - AQ$ was used. Here *sat* is a saturation period of 6 s with the saturation frequency equal to the HDO frequency. The $\tau$ delays were identical to those of the SERF experiment and the acquisition time, $AQ$, was 1.820 s.

Finally, the reliability of the relaxation rates obtained from the SERF experiment was verified by a comparison with the corresponding rates obtained from a conventional IR experiment. Three of the fast relaxing protons, namely His39 H$^{\alpha}$, His39 H$^{\delta_2}$, and His39 H$^{\varepsilon_1}$, are sufficiently well-resolved in a regular one-dimensional $^1$H spectrum to allow a determination of the relaxation rates from an IR experiment. As it appears from the comparison in Table 3, corresponding rates from the two experiments are identical within the uncertainties, thus confirming the reliability of the rates obtained from the SERF experiment. It should be noted that the SERF experiment results in more precise rates because of the higher resolution and the higher sensitivity of this experiment compared to the IR experiment.

## CONCLUSIONS

The SERF experiment presented here allows a selective measurement of the longitudinal relaxation rates of fast relaxing signals, while it suppresses slower relaxing signals. The range of relaxation rates of the observed and the suppressed signals, respectively, can be selected by an adjustment of the parameters $R_1^o$, $R_1^s$, and $c$. The applicability of the SERF experiment is demonstrated here by measuring the relaxation rates of a series of fast relaxing protons in a sample of partly oxidized *A.v.* PCu. However, by proper adjustment of the parameters $R_1^o$, $R_1^s$, and $c$, the SERF experiment can be used also in other cases where selective observation of signals with relaxation rates within a specific range of rates is required.

A UNIX/Linux computer program for calculating the variable delays $\Delta_1$ and $\Delta_2$ from the parameters $R_1^o$, $R_1^s$, $c$, $\tau$, and $t_a$ using Eqs. [7] and [14] is available from the authors.

## ACKNOWLEDGMENTS

Exploratory 800 MHz spectra were acquired at The Danish Instrument Centre for NMR Spectroscopy of Biological Macromolecules. We are grateful to Lixin Ma and Malene R. Jensen for helpful discussions, to Lise-Lotte Jespersen and Jens Ulstrup for providing the *A.v.* PCu samples, and to Else Philipp, Søren M. Kristensen, and Jens Duus for technical assistance. The study was financially supported by the Danish Natural Science Research Council (J. Nos. 9400351, 9502759, and 9801801), Direktør Ib Henriksens Fond and Novo Nordisk Fonden.

## REFERENCES

1. L. Ma and J. J. Led, Determination by high field NMR spectroscopy of the longitudinal electron relaxation rate in Cu(II) plastocyanin from *Anabaena variabilis*, *J. Am. Chem. Soc.* **122,** 7823–7824 (2000).
2. L. Ma, A.-M. M. Jørgensen, G. O. Sørensen, J. Ulstrup, and J. J. Led, Elucidation of the paramagnetic $R_1$ relaxation of heteronuclei and protons in Cu(II) plastocyanin from *Anabaena variabilis*, *J. Am. Chem. Soc.* **122,** 9473–9485 (2000).
3. I. Bertini, A. Donaire, C. Luchinat, and A. Rosato, Paramagnetic relaxation as a tool for solution structure determination: *Clostridium pasteurianum* Ferredoxin as an example, *Proteins: Struct. Funct. Genet.* **29,** 348–358 (1997).
4. S. L. Patt and B. D. Sykes, Water eliminated Fourier transform NMR spectroscopy, *J. Chem. Phys.* **56,** 3182–3184 (1972).
5. T. Inubushi and E. D. Becker, Efficient detection of paramagnetically shifted NMR resonances by optimizing the WEFT pulse sequence, *J. Magn. Reson.* **51,** 128–133 (1983).
6. L. Ma, E. Philipp, and J. J. Led, Determination of the electron self-exchange rates of blue copper proteins by super-WEFT NMR spectroscopy *J. Biomol. NMR* **19,** 199–208 (2001).
7. R. L. Vold, J. S. Waugh, M. P. Klein, and D. E. Phelps, Measurement of spin relaxation in complex systems, *J. Chem. Phys.* **48,** 3831–3832 (1968).
8. E. D. Becker, J. A. Ferretti, R. K. Gupta, and G. H. Weiss, The choice of optimal parameters for measurement of spin-lattice relaxation times. II. Comparison of saturation recovery, inversion recovery, and fast inversion recovery experiments, *J. Magn. Reson.* **37,** 381–394 (1980).
9. F. Bloch, Nuclear induction, *Phys. Rev.* **70,** 460–474 (1946).
10. U. Badsberg, A.-M. M. Jørgensen, H. Gesmar, J. J. Led, J. M. Hammerstad, L.-L. Jespersen, and J. Ulstrup, Solution structure of reduced plastocyanin from the blue–green alga *Anabaena variabilis*, *Biochemistry* **35,** 7021–7031 (1996).
11. D. S. Wishart and B. D. Sykes, Chemical shifts as a tool for structure determination, *Methods Enzymol.* **239,** 363–392 (1994).
12. R. Moss, H. Gesmar, and J. J. Led, A new linear prediction model method for the determination of slow amide proton exchange rates from series of one-dimensional $^1$H NMR spectra, *J. Am. Chem. Soc.* **116,** 747–749 (1994).
13. H. Gesmar and P. C. Hansen, "Fast" linear prediction and its application to NMR spectroscopy, *J. Magn. Reson. Ser. A* **106,** 236–240 (1994), doi:10.1006/jmre.1994.1030.
14. E. T. Adman, Structure and function of copper-containing proteins, *Curr. Opin. Struct. Biol.* **1,** 895–904 (1991).